Vol. 69: 113–122, 2013
doi: 10.3354/ame01626

AQUATIC MICROBIAL ECOLOGY
Aquat Microb Ecol

Published online May 28

FREE ACCESS

Changes in N cycling induced by *Ulva* detritus enrichment of sediments

Emilio García-Robledo[1,2,*], Niels Peter Revsbech[2], Nils Risgaard-Petersen[3], Alfonso Corzo[1]

[1]Dpto. Biología, Facultad de Ciencias del Mar y Ambientales, Universidad de Cádiz, Pol. Río San Pedro s/n. 11510, Puerto Real, Cádiz, Spain

[2]Section of Microbiology, and [3]Center for Geomicrobiology, Department of Bioscience, Aarhus University, 8000 Aarhus C, Denmark

ABSTRACT: Macroalgal accumulation and decomposition in shallow water environments typically result in an increase in the organic matter content of the sediment, affecting both benthic metabolism and nutrient dynamics. The present study investigates how a pulse addition of *Ulva* detritus to estuarine sediment influences the micro-distribution of O_2, NO_3^- and NO_2^- within the sediment, as well as the rates of oxygen consumption, nitrification and nitrate reduction. The micro-distributions of O_2, NO_3^- and NO_2^- were monitored with microsensors in *Ulva*-amended sediment microcosms and in unamended controls during a 1 mo incubation experiment. Process rates were obtained from numerical modeling of the concentration profiles. Oxygen consumption and nitrate reduction were enhanced by a factor of 2 in *Ulva*-amended sediment compared to the control. This led to a significant reduction in the penetration depths of oxygen and nitrate. Nitrification increased significantly in response to enhanced NH_4^+ supply from decomposition of the *Ulva* detritus. Aerobic ammonia oxidation exceeded rates of nitrite oxidation, leading to accumulation of NO_2^- in the oxic zone of the sediment. Nitrite and NO_3^- produced via nitrification diffused up to the sediment surface, inducing a net efflux to the water column, and downwards, supporting a high rate of denitrification coupled to nitrification. The present study shows that organic enrichment with *Ulva* detritus enhances sediment oxygen uptake, nitrification and denitrification, the net result being loss of nitrogen from the system. This might constitute a compensating or self-restoration mechanism counteracting an increase in N in intertidal sediment affected by eutrophication-induced macroalgal blooms.

KEY WORDS: Microbenthos · Denitrification · Nitrification · NO_X^- biosensors · Microelectrodes · Macroalgae · *Ulva* · Organic matter

INTRODUCTION

Massive growth and accumulation of green macroalgae is a worldwide phenomenon (Valiela et al. 1997, McGlathery et al. 2007). The increase in magnitude and frequency of these blooms is correlated to the high nutrient loadings and following eutrophication of coastal areas (Peckol & Rivers 1996). During blooms, high macroalgal densities can accumulate and decompose on top of coastal sediments and thereby heavily modify benthic communities. Decomposing accumulations of algae on the sediment surface induce increases in the carbon (C) and nitrogen (N) content of the sediment (Pihl et al. 1999, Corzo et al. 2009) and enhancements of benthic microbial metabolism (Trimmer et al. 2000, Lomstein et al. 2006). As a result, nutrient efflux from the sediment increases, favouring further growth of macroalgae and development of successive bloom events (Trimmer et al. 2000, Astill & Lavery 2001, Sundbäck et al.

*Email: emilio.garcia@uca.es

2003). This feedback effect has led to the hypothesis of 'self-perpetuating systems', where the high nutrient loading and the successive accumulation of macroalgae over years favour the appearance and growth of opportunistic macroalgae (Pihl et al. 1999, Tyler & McGlathery 2003).

The triggers of bloom collapses are still poorly defined. Therefore, it is difficult to predict the initiation of the bloom collapse and to follow the decomposition process and subsequent evolution of the benthic system. As a consequence, micro- and mesocosm approaches have been used instead to simulate and study the effects of decomposing macroalgae on benthic communities. Such a microcosm experiment was conducted by García-Robledo et al. (2008) who added frozen and thawed *Ulva* on top of a phototrophic intertidal sediment and recorded the following changes in sediment chemistry and metabolism (García-Robledo et al. 2008). The complete macroscopic decomposition of the macroalgal fronds led to increased pore water nutrient concentrations and subsequent growth of the microphytobenthic community (García-Robledo et al. 2008). Moreover, indirect evidence suggested an increase in nitrification and in coupled nitrification–denitrification as well (García-Robledo et al. 2008). The role and function of the nitrifying and denitrifying community during the decomposition of macroalgal detritus have a special interest in eutrophied areas frequently affected by macroalgal blooms. An enhancement of nitrification/denitrification activities in the sediment after a bloom collapse would favour the removal of nitrogen in a nutrient-enriched system and thereby constitute a type of self-restoration mechanism to reduce the eutrophication in those areas.

The aim of this study was to determine how decomposition of *Ulva* detritus affects nitrification, nitrate reduction and the distribution of NO_2^- and NO_3^- in the sediment, as well as the exchange of N between the sediment and the overlying water. The recently improved biosensors for NO_2^- and NO_X^- (NO_2^- + NO_3^-) (Revsbech & Glud 2009) and O_2 microsensors were used to measure the concentrations and spatial distributions of NO_2^-, NO_X^- and O_2 in *Ulva*-amended sediment microcosms and in unamended controls during a 1 mo incubation experiment. NO_X^- profiles were modelled to study the effects of *Ulva* detritus enrichment on the vertical distribution and magnitude of nitrification and anaerobic NO_X^- consumption. Integrated rates of the modelled processes, combined with measurement of sediment–water nutrient fluxes, were used to obtain the net nitrogen balance for the sediment with and without *Ulva* detritus. These results constitute the first study at a microscale of the distribution of NO_3^- and NO_2^- in sediments affected by detritus loading and contribute to determining the relative importance of the nitrification/denitrification processes occurring inside the sediments in areas affected by eutrophication-induced macroalgal blooms.

MATERIALS AND METHODS

Microcosm set-up

Surface sediment (upper 5 cm layer) was collected at 1 m water depth in Randers Fjord, Denmark, where high capacities for denitrification have been found (Nielsen et al. 2001). The sediment was sieved through a 1 mm screen in order to remove large animals and shell fragments. Planar *Ulva* (C:N ratio = 8.9) was collected from Norsminde Fjord, Denmark, dried at 80°C for 24 h and ground to a fine powder. Sediment was enriched with *Ulva* detritus (5 mg of *Ulva* powder per gram of sediment), resulting in an increase in the sediment carbon and nitrogen content of 1.1 and 0.2 mg g^{-1}, respectively (Table 1). After homogenisation, sediment was added to aquaria (245 × 150 × 150 mm, n = 3) to a depth of 8 cm (hereafter referred to as *Ulva* aquaria). A second set of aquaria (n = 3) filled with unamended sediment (control aquaria) was utilised.

Aquaria were filled with 1.8 l of artificial brackish water (10 psu salinity) creating a 5 cm water column above the sediment, placed in a water-filled tank at 15°C and covered with dark plastic. Artificial brackish water was prepared by diluting seawater collected at Aarhus Bay with tap water. Nitrate was added to the inflow water reservoir to maintain the *in situ* concentration of 100 µM in the aquaria throughout the experiment. An open water flow of 0.25 l h^{-1} (hydraulic retention time = 7 h) was set up in each aquarium using the same brackish water, letting the

Table 1. Organic matter (OM), organic carbon (OC), nitrogen (N) and C:N molar ratio in the control and *Ulva*-amended sediments. Data are means (±SE; n = 3)

	OM (mg g^{-1})	OC (mg g^{-1})	N (mg g^{-1})	C:N
Control	61.1 ± 0.2	27.99 ± 0.33	3.21 ± 0.05	10.17 ± 0.06
Ulva amended	64.8 ± 0.6	29.06 ± 0.10	3.40 ± 0.03	9.97 ± 0.06

water overflow the aquaria. To ensure complete water column mixing and avoid development of anoxic conditions, the water in each aquarium was gently purged with air.

Weekly sampling was performed over a 31 d period. On each sampling occasion, NO_X^-, NO_2^- and O_2 microprofiles and inorganic nutrient concentration in the aquaria and inflow water were measured in order to determine changes in oxygen and nitrogen metabolism and their effects on the net N balance of the sediments.

Water chemistry

Nutrient samples (5 ml, n = 3) were taken from the inflow water and inside the well-mixed aquaria on each sampling day, filtered through Whatman GF/F filters and stored frozen until analysis. The stirring conditions established in the water column ensured that the outflow water was equal to the water inside the aquaria. Concentrations of NO_X^- were measured using the vanadium chloride reduction method (Braman & Hendrix 1989) using a chemiluminescence NO analyzer (modelCLD 86, Eco Physics AG; Meyer et al. 2005). Nitrite and ammonium concentrations were determined by a standard colourimetric method described by Grasshoff et al. (1983). Nitrate was determined as the difference between NO_X^- and nitrite.

Ammonium, nitrate and nitrite fluxes in the aquaria were calculated using a mass balance approach. We estimated these fluxes from the difference in concentrations of the respective species in the in- and outflow water normalised by the flow rate and the sediment surface area. Nutrient fluxes were expressed as µmol m^{-2} h^{-1}.

Oxygen, NO_3^- and NO_2^- pore water profiles

Depth profiles of NO_X^-, NO_2^- and O_2 in the sediments were measured on each sampling day using microsensors for O_2 (Revsbech 1989b) and microscale biosensors for NO_X^- and NO_2^- (Nielsen et al. 2004, Revsbech & Glud 2009). Profiles of NO_3^- were calculated by subtracting the NO_2^- profile from the NO_X^- profile. Water column samples for NO_X^- and NO_2^-, were used to calibrate the sensors.

Oxygen, NO_X^- and NO_2^- sensors were mounted together on a computer controlled micromanipulator (MC-232, Unisense) with the tips in approximately the same vertical position and about 2 mm apart. Profiles of oxygen, NO_X^- and NO_2^- were measured simultaneously, and the signals were recorded using an A/D converter (ADC816, Unisense). Both motor and converter were connected to a computer and controlled by SensorTrace PRO software (Unisense).

Depth profiles of O_2, NO_X^-, NO_3^- and NO_2^- production/consumption were calculated from the respective concentration profiles using the PROFILE software (Berg et al. 1998). In the calculation of transformation rates, PROFILE applies an estimate of the diffusion coefficient of species in the sediment (D_s) based on the sediment porosity (ϕ) and the diffusion coefficient of the respective species at infinite dilution in water (D_w), both of which are required as input parameters. To get an exact value for D_s we determined the effective diffusion coefficient ($D_e = \phi \cdot D_s$) for O_2 from the steady state O_2 profile measured in mercury-inactivated sediment samples (Revsbech 1989a). Then we calculated ϕ assuming the following relationship: $D_s = \phi^2 D_w$ (Ullman & Aller 1982). Hence $\phi = (D_e/D_w)^{(1/3)}$. The calculated value for ϕ and diffusion coefficients for O_2, NO_X^-, NO_3^- and NO_2^- at infinite dilution (Boudreau 1997) were then used as input parameters for PROFILE, which in the given implementation used the relationship: $D_s = \phi^2 D_w$ as an estimate for D_s. Total nitrification and anaerobic NO_X^- consumption (ANC) were determined from the calculated production profiles (Meyer et al. 2001). ANC may include 3 NO_X^- reduction processes: denitrification, anaerobic ammonium oxidation (anammox) and dissimilatory nitrate reduction to ammonium (DNRA).

The relative importance of anammox was initially measured following the procedure described by Risgaard-Petersen et al. (2003), being as low as 0.5% of the total N_2 production (data not shown). DNRA could be a relevant process, but only under high organic matter loads (Christensen et al. 2000) and/or dominance of filamentous sulphide-oxidising bacteria (Sayama et al. 2005), which was not the case in the present experiment. Therefore, denitrification was most likely the main process contributing to the measured ANC rates (hereafter referred to as denitrification rates).

Statistical analysis

Differences between treatments, time and their combined effect (interaction) were tested by repeated-measures analysis of variance (RM ANOVA), followed by the Tukey honestly significant difference test for multiple pairwise comparisons. Data were $\log(x + 1)$ transformed if Shapiro-Wilk test for nor-

mality failed. Correlations between variables were also investigated using the software Statgraphics Centurion XVI or SigmaPlot 11.

RESULTS AND DISCUSSION

Experimental advantages and limitations

The causes triggering macroalgal bloom collapse and decomposition are not well defined and therefore are difficult to predict and measure *in situ*. The use of microcosms cannot reproduce the complex interactions occurring *in situ*, but allows simulation of the decomposition phase of a bloom under well-defined and controlled experimental conditions. The use of *Ulva* fronds, added directly to the sediment surface, creates large heterogeneities at a microscale (García-Robledo et al. 2008) which would require the measurement of a non-feasible number of NO_X^- and NO_2^- profiles to describe such spatial variability. In our experiment, macroalgal detritus was dried, powdered and mixed with sediment to obtain homogeneous detritus enrichment, being more appropriate for microsensor measurements. This simplified situation cannot be directly extrapolated then to the decomposition process of macroalgal fronds in the field. However, in areas affected by macroalgal blooms, the successive input of macroalgal detritus results in an organic matter increase in the first centimetres of the sediment (Pihl et al. 1999), similar to the simulated detritus enrichment performed in our experiment. The results shown in the present study represent a first description of the effects of organic matter loading on key processes of the N biogeochemical cycle at a microscale. These processes are affected by many environmental biotic and abiotic factors both *in situ* and in experimental set-ups, and all results will thus represent snapshots of outcomes from the given set of variables.

Effects of *Ulva* detritus enrichment on O_2 and NO_X^- sediment microprofiles

Clear differences in O_2, NO_X^- and NO_2^- profiles were observed in the *Ulva* detritus-amended sediment as compared to the controls (Figs. 1 & 2). Oxygen consumption was signifi-

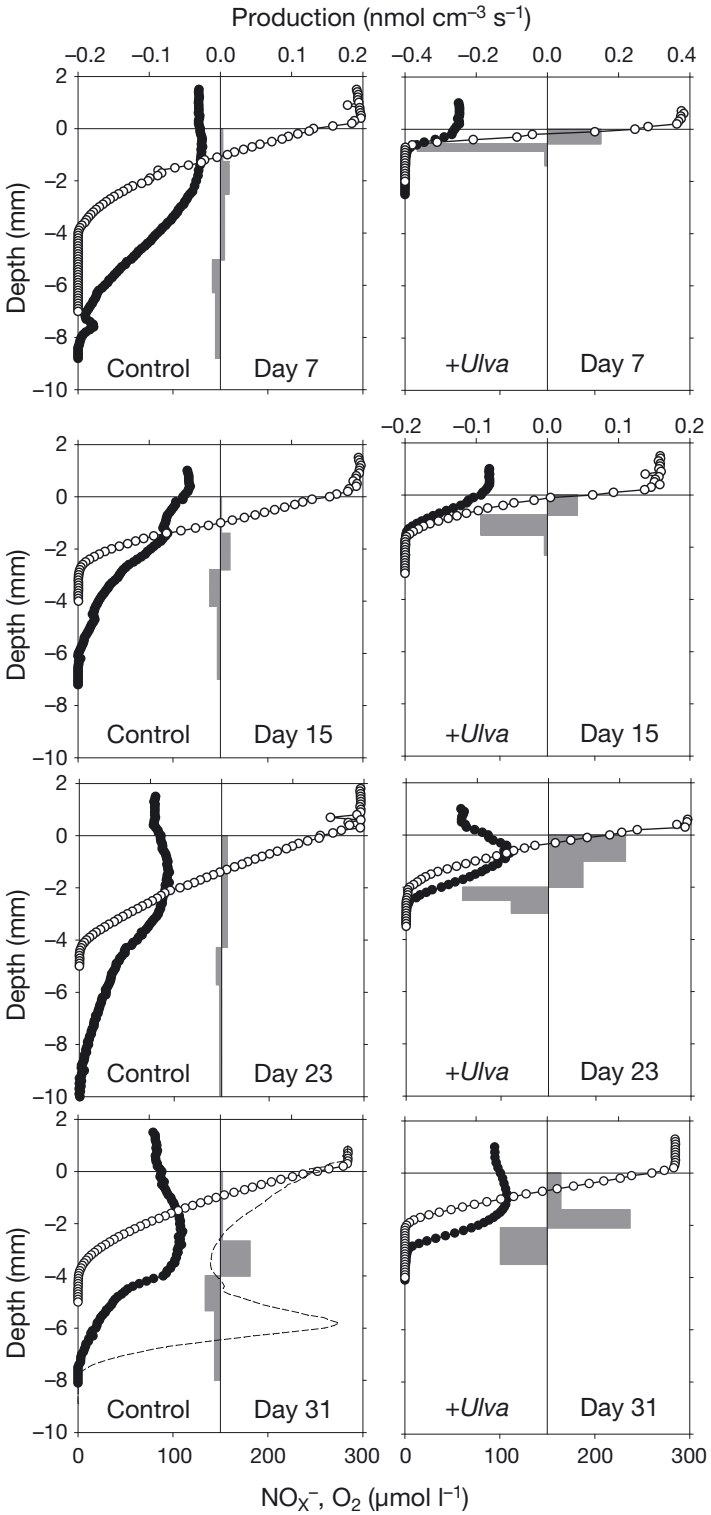

Fig. 1. Time evolution of NO_X^- (white dots) and O_2 (black dots) microprofiles in the control and *Ulva*-enriched aquaria. Production profiles obtained with numerical modelling of NO_X^- profiles (Berg et al. 1998) are shown as bars. Note the different scale used for Day 7 of the *Ulva*-enriched aquarium. An O_2 profile modified by bioturbation is shown for Day 31 of the control as well (dashed line). Data are representative profiles for each day

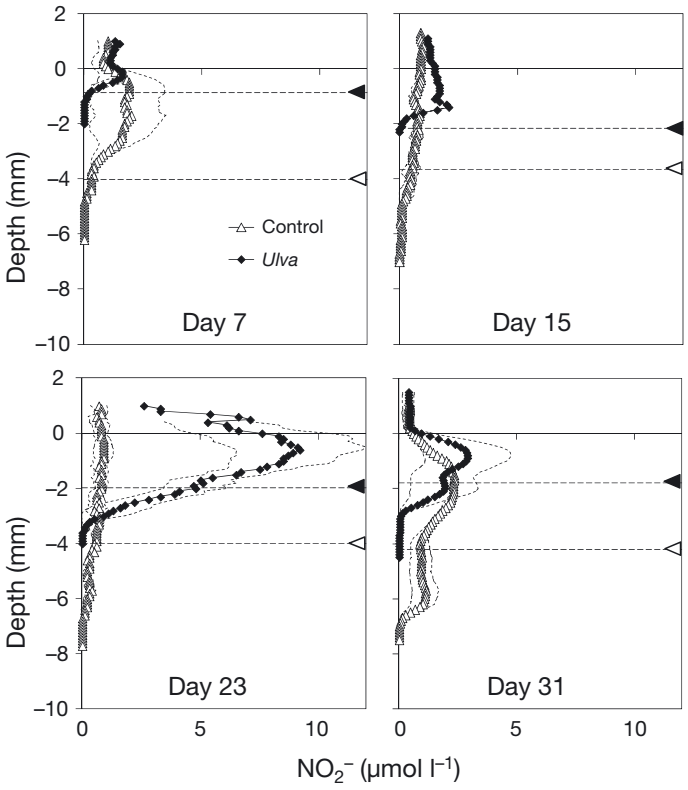

Fig. 2. Evolution of NO_2^- profiles in the control (white triangles) and *Ulva*-enriched (black diamonds) aquaria. Oxygen penetration depth is indicated by a horizontal dashed line marked with a black and white triangle for *Ulva*-amended and control sediment, respectively. Data are means of at least 3 profiles. Dashed lines following the plots represent the standard error

cantly enhanced in the *Ulva*-amended sediments as compared to the controls throughout the course of the experiment ($p < 0.05$, RM ANOVA) (Fig. 1). In general, oxygen consumption was 1.5 to 2.8 times higher than in the control, with no significant differences over time ($p > 0.05$, RM ANOVA) (Fig. 3A). This was similar to what has been found in other experimental studies of *Ulva*-enriched sediments (Lomstein et al. 2006, García-Robledo et al. 2008). The oxygen penetration depth increased from approximately 1 to 2 mm during the course of the experiment in the *Ulva*-amended sediment. This increase in oxygen penetration depth was probably due to depletion of carbon caused by a rapid decomposition of labile compounds released from the *Ulva* detritus during the first week of the experiment (Enríquez et al. 1993, Canfield et al. 2005). Oxygen penetration was constant in the control sediment at approximately 4 mm.

The addition of *Ulva* detritus caused pronounced changes in the nitrogen cycle of the sediment. Nitrate and NO_2^- profiles were significantly modified by *Ulva* detritus enrichment (Figs. 1 & 2). Throughout the first 2 wk, O_2 and NO_X^- were depleted within the upper 1 to 1.5 mm of the *Ulva*-amended sediment (Fig. 1). NO_2^- was only detected in the oxic zone, showing a small production peak (Fig. 2). The alignment of the sensors relative to the sediment surface was, however, not sufficiently precise to determine whether the consumption took place within the lowest part of the oxic layer (only 1 mm thick) or below the oxic/anoxic boundary. After Day 23, NO_X^- and NO_2^- production peaks developed in the first millimetre of the *Ulva* sediment, suggesting an increase in nitrification activity. This elevated NO_X^- production in combination with a general decrease in carbon oxidation activity caused NO_X^- penetration to increase down to approximately 3 mm below the sediment surface. The nitrite penetration depth also increased down to 3 mm, and (on Day 31) 2 production peaks could be detected, 1 in the oxic layer and 1 just below the oxic–anoxic interface. In contrast, NO_X^- and NO_2^- profiles did not change significantly during the experiment in the control sediments. A small NO_X^- production peak was observed in the oxic zone, and NO_X^- was consumed within the upper 2 to 5 mm anoxic layers of the sediment. The NO_X^- penetration depth varied from 6 to 9 mm, probably reflecting the spatial heterogeneity of the sediment. Except for Day 15, there was a peak of NO_2^- in the oxic layer of the sediment, indicating production by nitrification and net transport to both the overlying water and the anoxic layers of the sediment. At Day 31 there was a secondary peak of NO_2^- in the anoxic sediment at 6 mm depth, indicating net production in this layer by nitrate reduction.

The NO_X^- profiles were modelled to determine changes in the magnitude and distribution of the main microbial processes controlling nitrate and nitrite pore water concentrations and sediment–water fluxes (Fig. 1). For the *Ulva*-amended sediment, volumetric nitrification rates were highest during the first 2 wk, but were restricted to a narrow layer thinner than 1 mm. The depth-integrated nitrification rates were similar to those measured in control sediments ($p > 0.05$, post hoc Tukey test, RM ANOVA) (Fig. 3B). The progressive increase in O_2 penetration depth favoured the parallel increase in both magnitude and depth distribution of NO_X^- production compared to in the control sediment. Anoxic NO_X^- consumption was significantly enhanced in the *Ulva*-amended sediment compared to the control

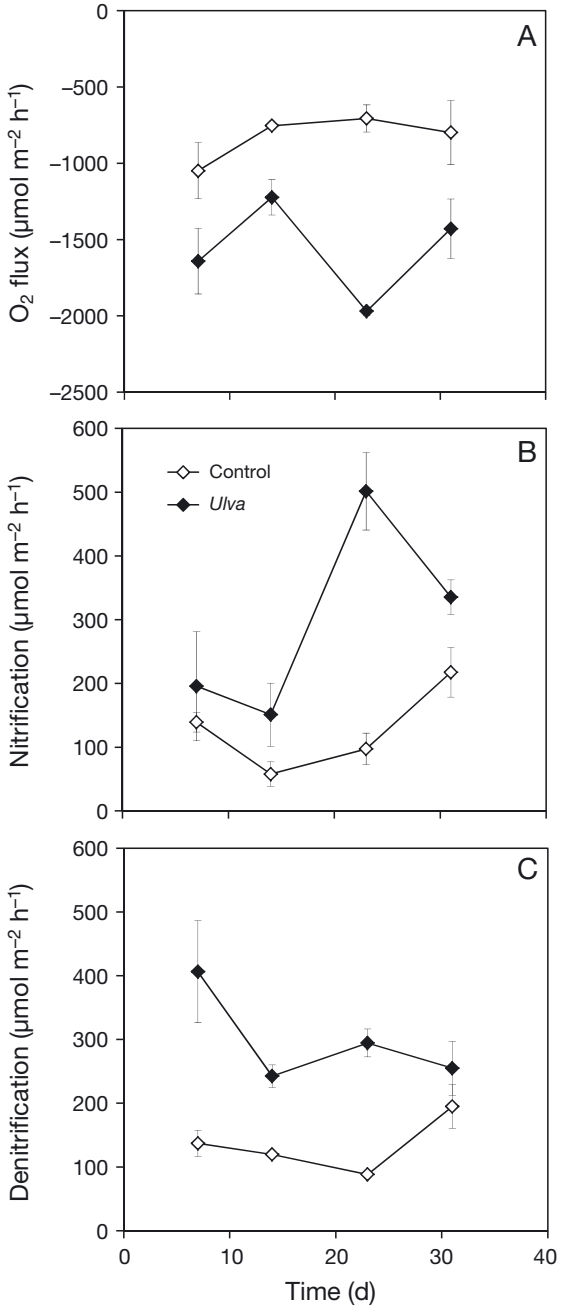

Fig. 3. (A) Sediment–water oxygen fluxes in the control and *Ulva* aquaria calculated from O_2 microsensor data. (B) Nitrification rates calculated as integration in depth of NO_X^- transformation rates in the oxic part of the sediment and (C) denitrification rates as the integration of consumption rates in the anoxic part of the sediment, both obtained by numerical modelling of NO_X^- profiles. Data are means (±SE; n = 3)

sediments ($p < 0.05$, RM ANOVA) (Fig. 3C). Nitrate was consumed in a narrow zone of 0.5 mm during the first week (Fig. 1), where O_2 penetration was <1 mm. Afterwards, volumetric anoxic consumption rates decreased progressively, while the width of the consumption zone increased, resulting in near constant denitrification rates (Fig. 3C).

Effects of *Ulva* detritus enrichment on nitrification

Oxygen and ammonium supplies to the surface layers, both essential for nitrification (Kemp et al. 1990, Caffrey et al. 1993, Rysgaard et al. 1994), changed significantly in the *Ulva*-amended sediments as compared to the control (Figs. 1 & 4). Mineralisation of *Ulva* detritus, with a low C:N ratio, increased the pore water NH_4^+ concentration as seen in previous studies (Trimmer et al. 2000, García-Robledo et al. 2008), resulting in a large efflux to the overlying water during the experiment (Fig. 4A). The higher NH_4^+ supply would stimulate the activity of ammonium-oxidising bacteria (AOB) and thus increase nitrification rates (Caffrey et al. 1993, Sloth et al. 1995). However, relatively low numbers of nitrifying bacteria as compared to heterotrophs may also contribute to initially low nitrification rates when organic matter is added (Nielsen & Revsbech 1998). In addition, the parallel enhancement of heterotrophic activity reduced the extension of the oxic layer during the first 2 wk (Fig. 1) and probably enhanced the competition for oxygen between the nitrifying community and heterotrophs. The high abundance of heterotrophic bacteria, added to the lower affinity of AOB for oxygen (Focht & Verstraete 1977, Prosser 1990, in Gieseke et al. 2001), limited nitrification activity (Fig. 1). Nitrite-oxidising bacteria (NOB) have even lower affinity for oxygen than AOB (Schramm 2003), possibly contributing to a slight nitrite accumulation in the oxic zone (Fig. 2). The overall result of the aforementioned processes was that nitrification rates were similar to control sediment, despite the higher ammonium availability during the first 2 wk (Fig. 3B).

Efficient decomposition of labile organic carbon from *Ulva* amendments during the initial phases of the experiment led to reduced O_2 consumption and elevated O_2 penetration during the second half of the experiment (Fig. 1). The increase in oxygen availability favoured the growth and activity of the nitrifying community, as evidenced by a pronounced NO_X^- production peak in the *Ulva*-amended sediment on Days 23 and 31 and an increase in the depth penetration of NO_X^- (Fig. 1). This resulted in significant increase in nitrification rates compared to the first 2 wk in *Ulva*-amended and control sediment ($p < 0.05$, post hoc Tukey test, RM ANOVA) (Fig. 3). An imbalance

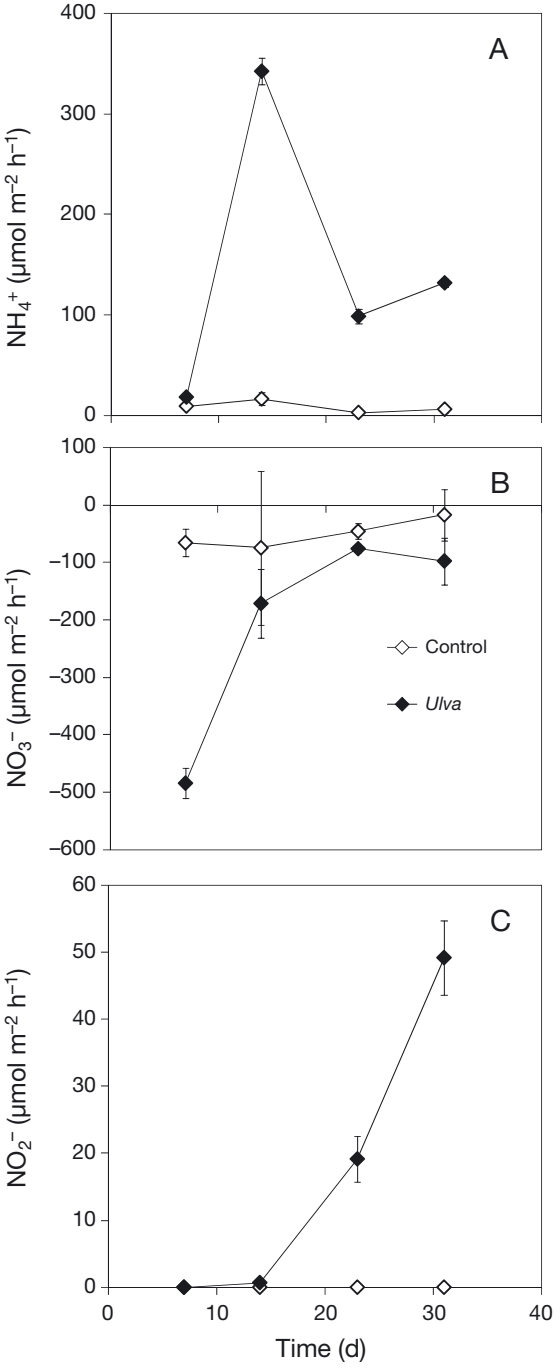

Fig. 4. Net inorganic nitrogen fluxes in aquaria: (A) ammonium, (B) nitrate and (C) nitrite. Net fluxes were measured as the difference between inflow and outflow and normalised by flow rate and area. Data are means (±SE; n = 3)

between AOB and NOB activities resulted in a rarely reported nitrite peak in the oxic part of the sediment (Fig. 2) (Cooke & White 1987, Davidsson et al. 1997, De Beer et al. 1997, Stief et al. 2002). A fraction of the accumulated NO_2^- diffused into the water column, transforming *Ulva*-amended sediment into a net NO_2^- source. In contrast, NO_2^- was found at low concentrations in both oxic and anoxic parts of the control sediments, indicating that AOB and NOB activities were balanced and no NO_2^- was detected in the water column.

Effects of *Ulva* detritus enrichment on denitrification

Among the factors that influence denitrification rates, availability of electron donors, depth of the oxic–anoxic interface and nitrification rates are considered the most important (Christensen et al. 1990, Rysgaard et al. 1994, Piña-Ochoa & Alvarez-Cobelas 2006). In the present experiment, the reduction of the oxygen penetration depth in *Ulva*-amended sediment reduced the diffusive distance between water column NO_X^- and the oxic–anoxic interface, favouring denitrification supported by water column NO_X^-. As a result, we found a significant inverse correlation between oxygen penetration depth and NO_3^- influx ($r = -0.71$, $p < 0.01$, Pearson correlation). During the first 2 wk, the oxygen penetration depth was minimal and denitrification rates exceeded nitrification rates by factors of 1.5 to 2 (Fig. 3, Table 2). NO_X^- being produced by nitrification or coming

Table 2. Nitrogen budget of the sediment–water nutrient fluxes and nitrification (Ni) and denitrification (DNi) rates obtained by NO_X^- microprofiles in the control and *Ulva*-amended sediments. Total dissolved inorganic nitrogen (DIN) flux was calculated as the sum of nitrate, nitrite and ammonium fluxes. Net NO_X^- is the net production/consumption rate calculated from the NO_X^- profiles (Ni – DNi). Rates are expressed as mmol m^{-2} d^{-1}. Data were integrated throughout the experimental period (Days 7 to 31) to get average daily values from Day 7 to 31

Day	Water flux balance				NO_X^- profiles		
	NO_3^-	NO_2^-	NH_4^+	Total DIN flux	Ni	DNi	Net NO_X^-
Control							
7	−1.6	0.0	0.2	−1.3	3.3	3.3	0.0
15	−1.8	0.0	0.4	−1.4	1.4	2.9	−1.5
23	−1.1	0.0	0.1	−1.0	2.3	2.1	0.2
31	−0.4	0.0	0.1	−0.3	5.2	4.7	0.5
Average	−1.3	0.0	0.2	−1.1	2.7	3.0	−0.3
+Ulva							
7	−11.6	0.0	0.4	−11.2	4.7	9.8	−5.1
15	−4.1	0.0	8.2	4.1	3.6	5.8	−2.2
23	−1.8	0.5	2.4	1.0	12.0	7.1	5.0
31	−2.3	1.2	3.2	2.0	8.1	6.1	1.9
Average	−4.3	0.4	4.1	0.2	7.3	6.9	0.4

from the water column was consumed within the first 2 mm of the *Ulva*-amended sediment (Fig. 1). After Day 23, the increase in O_2 penetration depth and nitrification rates displaced the NO_X^- reduction zone deeper in the sediment. The consumption of NO_3^- coming from the water column decreased progressively (Fig. 4B), and the high denitrification rates were maintained by diffusion of NO_X^- produced by nitrification (Fig. 3). The typical net production profiles measured on Days 23 and 31 (Fig. 1) suggest a net diffusive NO_X^- release from the sediment. However, NO_3^- flux in the *Ulva*-amended aquaria was directed from the water towards the sediment, according to the net fluxes in aquaria (Fig. 4B). This indicates that at the whole-microcosm scale, the sediment was a sink of NO_3^- instead of a source, as suggested by the NO_X^- microprofiles (Fig. 4). The burrowing activity of small infauna growing in the aquaria (polychaetes and amphipods) may have increased the advective transport of nitrate to the sediment, resulting in localised net consumption of NO_3^- in the microcosms (Risgaard-Petersen et al. 2004, Nizzoli et al. 2007). Such transport was not implemented in the model used for interpretation of the concentration profiles, and our model estimates of consumption/production are therefore underestimates. Presence of infaunal activity was indicated in some of the O_2 profiles (see Fig. 1, control panel, Day 31). The ventilating activity of infauna may increase the O_2 concentration in the burrows (approximately 6 mm depth in the example profile) to values approaching those in the water column. Similarly, NO_X^- from the water column was also pumped into the sediment, resulting in an enhancement of NO_X^- consumption from the water column.

Effect of *Ulva* detritus enrichment on N cycling

The integration of the rates during the whole experiment (Day 7 to 31) illustrated the net result of the *Ulva* addition to the sediment (Table 2). Time-integrated rates (mmol m^{-2}) were normalised by the experiment duration (24 d) in order to obtain comparable daily rates. The overall process of *Ulva* detritus decomposition enhanced benthic metabolism, increasing the uptake of both O_2 and NO_3^- coming from the water column. The resulting nutrient remineralisation released large amounts of NH_4^+ to the pore water. This NH_4^+ enrichment of the pore water led to (1) activation of the nitrifying community by about 3-fold compared to the control and (2) increased NH_4^+ efflux to the water column by about 20-fold compared to the control. The organic matter enrichment coupled with a decrease in O_2 penetration caused enhancement of denitrification that reached up to 6.9 mmol m^{-2} d^{-1} in *Ulva*-amended sediment, about 2 times higher than in the control sediment. A net NO_X^- release to the water column (0.4 mmol m^{-2} d^{-1}) could be calculated from the microprofiles, whereas the microcosm mass balance showed net NO_X^- consumption in *Ulva*-amended sediment. The presence of infauna apparently increased the NO_x^- flux into the sediment, producing significant net consumption in *Ulva*-amended sediments (4.3 mmol m^{-2} d^{-1}), 3 times higher than that in controls (1.3 mmol m^{-2} d^{-1}). Nitrification apparently did not increase sufficiently to oxidise all NH_4^+ diffusing towards the sediment surface and burrows, resulting in the liberation of NH_4^+ to the water column. This release of N in the form of NH_4^+ was almost compensated by the uptake of NO_X^- from the water column at similar rates, but the total dissolved inorganic nitrogen mass balance of the sediment changed from negative in the control to slightly positive (Table 2). The fact that *Ulva*-amended sediment was a net source of NH_4^+ for the water column might have ecological implications for primary producers in the field, since NH_4^+ assimilation is energetically cheaper than that of NO_X^-.

In field studies, where macroalgae accumulate on top of the sediment, the oxygen penetration depth is permanently reduced (Corzo et al. 2009), leading to a low activity level of nitrifiers and coupled nitrification–denitrification (Trimmer et al. 2000) and a release of NH_4^+ from the sediment (Lomstein et al. 2006, García-Robledo et al. 2008). No field studies have previously shown the effects of enrichment in macroalgal detritus on the N cycle at a microscale within the sediment. The hypothesis of self-perpetuating systems suggests that the organic matter enrichment of the sediment produces a large nutrient regeneration supporting the subsequent macroalgal bloom. However, the results obtained in the present study show that, although the regeneration of nutrients from *Ulva* detritus integrated into the sediment does occur and leads to the release of NH_4^+, the eutrophication effect of this is counteracted by stimulation of coupled nitrification–denitrification and also denitrification, consuming large amounts of NO_3^- from the water column. The enhancement of the activity by nitrifying and denitrifying communities after macroalgal collapse constitutes a compensating or self-restoring mechanism in sediments affected by macroalgal blooms.

Acknowledgements. The research was funded by the Danish National Research Foundation, the German Max Planck Society and the following grants: CTM 2009-10736 (Ministry of Education and Science, Spain), P06-RNM-01787 (Andalusian Regional Government) and 10-083140 (Danish Natural Science Research Council). E. García-Robledo was funded by FPU Grant AP2005-4897 from the Ministry of Education and Science (Spain) and the Ramon Areces Foundation (Spain).

LITERATURE CITED

Astill H, Lavery PS (2001) The dynamics of unattached benthic macroalgal accumulations in the Swan-Canning estuary. Hydrol Processes 15:2387–2399

Berg P, Risgaard-Petersen N, Rysgaard S (1998) Interpretation of measured concentration profiles in sediment pore water. Limnol Oceanogr 43:1500–1510

Boudreau BP (1997) Diagenetic models and their interpretation: modelling transport and reactions in aquatic sediments. Springer, Berlin

Braman RS, Hendrix SA (1989) Nanogram nitrite and nitrate determination in environmental and biological materials by vanadium(III) reduction with chemiluminescence detection. Anal Chem 61:2715–2718

Caffrey JM, Sloth NP, Kaspar HF, Blackburn TH (1993) Effect of organic loading on nitrification and denitrification in a marine sediment microcosm. FEMS Microbiol Ecol 12:159–167

Canfield DE, Thamdrup B, Kristensen E (2005) Aquatic geomicrobiology. Elsevier Academic Press, London

Christensen PB, Nielsen LP, Sorensen J, Revsbech NP (1990) Denitrification in nitrate-rich streams: diurnal and seasonal variation related to benthic oxygen metabolism. Limnol Oceanogr 35:640–651

Christensen PB, Rysgaard S, Sloth NP, Dalsgaard T, Schwaerter S (2000) Sediment mineralization, nutrient fluxes, denitrification and dissimilatory nitrate reduction to ammonium in an estuarine fjord with sea cage trout farms. Aquat Microb Ecol 21:73–84

Cooke JG, White RE (1987) The effect of nitrate in stream water on the relationship between gentrification and nitrification in a stream-sediment microcosm. Freshw Biol 18:213–226

Corzo A, Van Bergeijk SA, García-Robledo E (2009) Effects of green macroalgal blooms on intertidal sediments: net metabolism and carbon and nitrogen contents. Mar Ecol Prog Ser 380:81–93

Davidsson TE, Stepanauskas R, Leonardson L (1997) Vertical patterns of nitrogen transformations during infiltration in two wetland soils. Appl Environ Microbiol 63: 3648–3656

De Beer D, Schramm A, Santegoeds C, Kuhl M (1997) A nitrite microsensor for profiling environmental biofilms. Appl Environ Microbiol 63:973–977

Enríquez S, Duarte CM, Sand-Jensen K (1993) Patterns in decomposition rates among photosynthetic organism: the importance of detritus C:N:P content. Oecologia 94: 457–471

Focht DD, Verstraete W (1977) Biochemical ecology of nitrification and denitrification. Adv Microb Ecol 1:135–214

García-Robledo E, Corzo A, Garcia de Lomas J, Van Bergeijk SA (2008) Biogeochemical effects of macroalgal decomposition on intertidal microbenthos: a mesocosm experiment. Mar Ecol Prog Ser 356:139–151

Gieseke A, Purkhold U, Wagner M, Amann R, Schramm A (2001) Community structure and activity dynamics of nitrifying bacteria in a phosphate-removing biofilm. Appl Environ Microbiol 67:1351–1362

Grasshoff K, Ehrhardt M, Kremling K (1983) Methods of sea water analysis, Vol 1. Verlag Chemie, New York, NY

Kemp WM, Sampoo P, Caffrey JM, Mayer M (1990) Ammonium recycling versus denitrification in Chesapeake Bay sediments. Limnol Oceanogr 35:1545–1563

Lomstein BA, Guldberg LB, Neubauer ATA, Hansen J and others (2006) Benthic decomposition of *Ulva lactuca*: a controlled laboratory experiment. Aquat Bot 85:271–281

McGlathery KJ, Sundbäck K, Anderson IC (2007) Eutrophication in shallow coastal bays and lagoons: the role of plants in the coastal filter. Mar Ecol Prog Ser 348:1–18

Meyer RL, Kjaer T, Revsbech NP (2001) Use of NO_x^- microsensors to estimate the activity of sediment nitrification and NO_x^- consumption along an estuarine salinity, nitrate, and light gradient. Aquat Microb Ecol 26: 181–193

Meyer RL, Risgaard-Petersen N, Allen DE (2005) Correlation between anammox activity and microscale distribution of nitrite in a subtropical mangrove sediment. Appl Environ Microbiol 71:6142–6149

Nielsen K, Risgaard-Petersen N, Sømod B, Rysgaard S, Bergø T (2001) Nitrogen and phosphorus retention estimated independently by flux measurements and dynamic modelling in the estuary, Randers Fjord, Denmark. Mar Ecol Prog Ser 219:25–40

Nielsen M, Larsen LH, Jetten MSM, Revsbech NP (2004) Bacterium-based NO_2^- biosensor for environmental applications. Appl Environ Microbiol 70:6551–6558

Nielsen TH, Revsbech NP (1998) Nitrification, denitrification, and N-liberation associated with two types of organic hot-spots in soil. Soil Biol Biochem 30:611–619

Nizzoli D, Bartoli M, Cooper M, Welsh DT, Underwood GJC, Viaroli P (2007) Implications for oxygen, nutrient fluxes and denitrification rates during the early stage of sediment colonisation by the polychaete *Nereis* spp. in four estuaries. Estuar Coast Shelf Sci 75:125–134

Peckol P, Rivers JS (1996) Contribution by macroalgal mats to primary production of a shallow embayment under high and low nitrogen-loading rates. Estuar Coast Shelf Sci 43:311–325

Pihl L, Svenson A, Moksnes P, Wennhage H (1999) Distribution of green algal mats throughout shallow soft bottoms of the Swedish Skagerrak archipelago in relation to nutrient sources and wave exposure. J Sea Res 41: 281–294

Piña-Ochoa E, Alvarez-Cobelas M (2006) Denitrification in aquatic environments: a cross-system analysis. Biogeochemistry 81:111–130

Prosser JI (1990) Autotrophic nitrification in bacteria. Adv Microb Physiol 30:125–181

Revsbech NP (1989a) Diffusion characteristics of microbial communities determined by use of oxygen microsensors. J Microbiol Methods 9:111–122

Revsbech NP (1989b) An oxygen microelectrode with a guard cathode. Limnol Oceanogr 34:474–478

Revsbech NP, Glud RN (2009) Biosensor for laboratory and lander-based analysis of benthic nitrate plus nitrite distribution in marine environments. Limnol Oceanogr Methods 7:761–770

Risgaard-Petersen N, Nielsen LP, Rysgaard S, Dalsgaard T, Meyer RL (2003) Application of the isotope pairing tech-

nique in sediments where anammox and denitrification coexist. Limnol Oceanogr Methods 1:63–73

Risgaard-Petersen N, Meyer RL, Schmid M, Jetten MSM, Enrich-Prast A, Rysgaard S, Revsbech NP (2004) Anaerobic ammonium oxidation in an estuarine sediment. Aquat Microb Ecol 36:293–304

Rysgaard S, Risgaard-Petersen N, Sloth NP, Jensen K, Nielsen LP (1994) Oxygen regulation of nitrification and denitrification in sediments. Limnol Oceanogr 39: 1643–1652

Sayama M, Risgaard-Petersen N, Nielsen LP, Fossing H, Christensen PB (2005) Impact of bacterial NO_3^- transport on sediment biogeochemistry. Appl Environ Microbiol 71:7575–7577

Schramm A (2003) *In situ* analysis of structure and activity of the nitrifying community in biofilms, aggregates, and sediments. Geomicrobiol J 20:313–333

Sloth NP, Blackburn H, Hansen LS, Risgaard-Petersen N, Lomstein BA (1995) Nitrogen cycling in sediments with different organic loading. Mar Ecol Prog Ser 116: 163–170

Stief P, Beer D, Neumann D (2002) Small-scale distribution of interstitial nitrite in freshwater sediment microcosms: the role of nitrate and oxygen availability, and sediment permeability. Microb Ecol 43:367–378

Sundbäck K, Miles A, Hulth S, Pihl L, Engström P, Selander E, Svenson A (2003) Importance of benthic nutrient regeneration during initiation of macroalgal blooms in shallow bays. Mar Ecol Prog Ser 246:115–126

Trimmer M, Nedwell DB, Sivyer DB, Malcom SJ (2000) Seasonal organic mineralisation and denitrification in intertidal sediments and their relationship to the abundance of *Enteromorpha* sp. and *Ulva* sp. Mar Ecol Prog Ser 203: 67–80

Tyler AC, McGlathery KJ (2003) Benthic algae control sediment–water column fluxes of organic and inorganic nitrogen compounds in a temperate lagoon. Limnol Oceanogr 48:2125–2137

Ullman WJ, Aller RC (1982) Diffusion coefficients in nearshore marine sediments. Limnol Oceanogr 27:552–556

Valiela I, McClelland J, Hauxwell J, Behr PJ, Hersh D, Foreman K (1997) Macroalgal blooms in shallow estuaries: controls and ecophysiological and ecosystem consequences. Limnol Oceanogr 42:1105–1118

Editorial responsibility: Rutger de Wit, Montpellier, France

Submitted: October 16, 2012; Accepted: March 13, 2013
Proofs received from author(s): April 30, 2013